Published in Journal of Hydrology 546, 16-27, 2017
which should be used for any reference to this work

# Infiltration under snow cover: Modeling approaches and predictive uncertainty

Jessica Meeks *, Christian Moeck, Philip Brunner, Daniel Hunkeler

*University of Neuchâtel, Neuchâtel 2000, Switzerland*

*Keywords:*
Uncertainty
Snowmelt
Energy balance
Day degree
Recharge
Karst
Groundwater

A B S T R A C T

Groundwater recharge from snowmelt represents a temporal redistribution of precipitation. This is extremely important because the rate and timing of snowpack drainage has substantial consequences to aquifer recharge patterns, which in turn affect groundwater availability throughout the rest of the year. The modeling methods developed to estimate drainage from a snowpack, which typically rely on temporally-dense point-measurements or temporally-limited spatially-dispersed calibration data, range in complexity from the simple degree-day method to more complex and physically-based energy balance approaches. While the gamut of snowmelt models are routinely used to aid in water resource management, a comparison of snowmelt models' predictive uncertainties had previously not been done. Therefore, we established a snowmelt model calibration dataset that is both temporally dense and represents the integrated snowmelt infiltration signal for the Vers Chez le Brandt research catchment, which functions as a rather unique natural lysimeter. We then evaluated the uncertainty associated with the degree-day, a modified degree-day and energy balance snowmelt model predictions using the null-space Monte Carlo approach. All three melt models underestimate total snowpack drainage, underestimate the rate of early and midwinter drainage and overestimate spring snowmelt rates. The actual rate of snowpack water loss is more constant over the course of the entire winter season than the snowmelt models would imply, indicating that mid-winter melt can contribute as significantly as springtime snowmelt to groundwater recharge in low alpine settings. Further, actual groundwater recharge could be between 2 and 31% greater than snowmelt models suggest, over the total winter season. This study shows that snowmelt model predictions can have considerable uncertainty, which may be reduced by the inclusion of more data that allows for the use of more complex approaches such as the energy balance method. Further, our study demonstrated that an uncertainty analysis of model predictions is easily accomplished due to the low computational demand of the models and efficient calibration software and is absolutely worth the additional investment. Lastly, development of a systematic instrumentation that evaluates the distributed, temporal evolution of snowpack drainage is vital for optimal understanding and management of cold-climate hydrologic systems.

## 1. Introduction

Infiltration resulting from snowmelt represents the temporal redistribution of liquid precipitation. This is extremely important because the rate and timing of snowpack drainage has substantial consequences to aquifer recharge patterns, which in turn affect groundwater availability throughout the rest of the year. In spite of its significance, direct measurement and modeling of snowpack outflow remains challenging due to the inherent limitations of monitoring instrumentation.

A number of field methods have been used to measure water drainage from snow packs (loss of snow water equivalence, SWE) including snow pillows (Archer and Stewart, 1995; Butcher and McManamon, 2011; Trujillo and Molotch, 2011), and snowmelt lysimeters (Jost et al., 2012; Kattelmann, 1989, 2000; Tekeli et al., 2005), both of which can render temporally dense point data. Extrapolation throughout a watershed of point measurements such as these is difficult due to the considerable spatial variability that exists in both snow depth and corresponding SWE and heterogeneous infiltration processes resulting from different soil types and structures across a watershed. Further, snow lysimeters have structural configurations that impose bias to the output data, such as sidewalls which are used to mitigate gains or losses from lateral

* Corresponding author.
*E-mail address:* Jessica.meeks@unine.ch (J. Meeks).

flow within a snowpack (Haupt, 1969; Martinec, 1986). Snow pillow data can also be skewed due to snow bridging. Snow courses (Marks et al., 2001; Rice and Bales, 2010) produce a more distributed understanding of SWE, however they are highly laborious and are typically done at a coarse time resolution. Assessment of SWE evolution is further complicated when considering that spatial variability in recharge from snowmelt also results from irregularity in the amount of water released from the base of the snowpack. This ensues from complicated, preferential pathways in which melt water travels through a snowpack before percolating to the base (Kattelmann, 1989). Ultimately, snow hydrologists still must rely on limited and possibly biased field data to obtain basic liquid inputs for snowmelt modeling (DeWalle and Rango, 2008).

Numerous modeling methods have been developed to evaluate snow processes, with complexities ranging between simple index models and physically based multi-layer models which simulate a snowpack's energy balance (Etchevers et al., 2004). The ongoing debate regarding the relative merits of these modeling end members (Franz et al., 2010) has manifested in several model intercomparisons (Feng et al., 2008; Magnusson et al., 2011; Rutter et al., 2009). In its simplest form, the degree-day (DD) method of modeling snowmelt is based on the assumption that snowmelt during a time interval is proportional to positive air temperature, with the proportionality factor being the degree-day factor C (Hock, 1999), an association first presented in (Linsley, 1943). The relative contributions of the different energy balance components can shift in space and time affecting the parameter C. These changes include cloud cover, snowpack conditions, shift in season or progression of day, aspect, slope and vegetation cover (Hock, 2003). That withstanding, Ohmura (2001) was able to show the computational validity of melt rate parameterization using air temperature, and that the degree-day method "works" because temperature information is transferred to earth's surface mainly through long wave atmospheric radiation, which is by far the most important heat source for melt. Several studies have demonstrated improvements to the DD method via incorporation of solar radiation (Hock, 1999, 2003; Jost et al., 2012) and progression of day (Tobin et al., 2013). Overall though, the efficacy of this index method is usually attributed to the way in which air temperature effectively integrates the influence of a range of meteorological variables, or energy fluxes (Hodgkins et al., 2012). Acquiring air temperature data is relatively easy and inexpensive. In contrast, more rigorous energy balance models are data intensive and usually require expensive instrumentation. At a minimum, physically based assessments take into account air temperature, relative humidity, wind speed, precipitation, global and incoming long wave radiation. With this breadth of information researchers can explicitly model changes in heat storage of a snowpack and solve for snow surface temperature using a heat budget formula (Jost et al., 2012), thereby more concisely modeling accumulation and ablation. The physics behind the energy balance method has been well documented (Anderson, 1968; Cline, 1995; Herrero et al., 2009; Male and Gray, 1981; Marks and Dozier, 1992). An exhaustive overview of snow models is presented by Yang (2008) and updated regularly on the Snow Modelers Internet Platform.

Choice of modeling method is in part dictated by data and computational availability. The empirical degree-day method requires little data and is easily applied in distributed modeling efforts, but does not explicitly take into consideration climatic forcing functions operating during snow accumulation and ablation. In contrast, the computationally intensive physically-based energy balance methods offers more insight into the processes controlling the energy balance (Hodgkins et al., 2012) but requires vast amounts of data, which in consequence hinders distributed application, needed for up-scaling of point-processes. Further, uncertainty may be introduced when adopted model parameters are unknown. Thus, to some degree, these modeling end members serve different needs within the modeling community.

Most numerical models are employed to aid in environmental management, and as such the uncertainty associated with predictions made by such models must be assessed (Gallagher and Doherty, 2007; Jost et al., 2012). However, given the issues with the above-discussed field methods for collection of calibration data and the lack of data for comparison, it has been difficult to quantify 1. to what extent these branches of snowmelt models provide robust estimates of snowpack outflow and 2. how well these models perform at different time scales. That said initial attempts on this front have been made. Seibert (1997) examined parameter uncertainty within the HBV model using a Monte Carlo approach. Since ranges in parameters can provide an almost equally good model fit, Seibert concluded that model predictions should be given a probability distribution rather than a single value, which is in keeping with assertions made by Melching et al. (1990) and Beven and Binley (1992). Franz et al. (2010) applied the Bayesian Model Averaging (BMA) method to an ensemble of twelve snow models, that varied in their heat and melt algorithms, parameterization, and/or albedo estimation method, to quantify the uncertainty associated with these sources of error in the stream flow forecasting process associated with snowmelt. Here the individual models BMA predictive mean, and BMA predictive variance were evaluated. An individual snow model would often outperform the BMA predictive mean. However, observed snow water equivalent was captured within the 95% confidence intervals of the BMA variance on average 80% of the time. Franz et al. concluded that consideration of multiple snow structures would provide useful uncertainty information for probabilistic hydrologic prediction. Slater et al. (2013) investigated uncertainty surrounding SWE reconstruction, when using remote sensing, and found that errors in model forcing data were at least as important, if not more so, than image availability when reconstructing SWE. Even though a few isolated studies have look at uncertainties surround snow processes models, uncertainty assessment of model performance is not routinely quantified for recharge estimates associated with snowmelt. So far, there have been no systematic comparisons of the uncertainties arising from different snowmelt modeling approaches at either the parametric or structural levels.

This paper presents a comparison of three snow-process models' ability to predict recharge from snowmelt and a short discussion pertaining to the application of these results at different temporal scales. This study was not intended to be an exhaustive analysis of either parameters nor model structure uncertainty but rather help shed light on how well snow process models are able to predict recharge, either at the event or seasonal scale. To generate snowmelt model calibration data, we used a large and natural lysimeter as proposed by Kattelmann (2000). This researcher stated that snowmelt runoff from a larger "natural lysimeter", a well defined catchment with an easily-monitored drainage point, would provide a conceptually better basis for evaluating output from snowmelt models than the somewhat artificial sampling of snowpack outflow by lysimeters and snow pillows. In following, the karstified Vers Chez les Brant (VCB), which can be viewed as an oversized, real-world lysimeter, consists of a 1600 $m^2$ watershed that drains infiltrating water to a cave discharge point (VCB1) 53 m below the ground surface (Meeks and Hunkeler, 2015). We used this rather unique natural lysimeter to evaluate the uncertainty surrounding modeled snowmelt predictions. We used a simple, albeit physically based vadose zone model, to back calculate snowmelt from the observed cave drainage. The back-calculated snowmelt does not retain any of the aforementioned data biases imposed by traditional lysimeters or snow pillows, has a fine time resolution, and represents the integrated behavior of snowmelt across the VCB recharge zone. This

back-calculated snowmelt data was then used as a point of comparison for the snow process models' predictions of time-series snowmelt data. The uncertainty associated with each model's recharge prediction was then systematically quantified through a rigorous calibration process, something that had yet to be undertaken by the snow modeling community. A visual workflow of these modeling efforts is included as Fig. 1.

## 2. Study area

The Vers Chez le Brandt (526450/199010 UPS) research site is situated within the 130 $km^2$ karstified Areuse Catchment in the Swiss Jura Range's western edge (Fig. 2). Upper Jurassic (Portlandian, Kimmeridgian and Sequanian) aged marl and fossiliferous limestone (Sommaruga, 1997; Valley, 2002) make up the region's bedrock and house the site's single chamber karst cavity. Up to 70 cm of Neolovisol loess soils blanket the autochthonous, solutionally altered bedrock (Havlicek, 1999) and are composed of two mineral systems that collectively make up the soil and epikarst, which are approximately 2 m in thickness (Elouardi, 1998; Müller, 1978). Based on field observations of VCB pedology and lithology, in conjunction with analysis of precipitation, soil moisture and VCB1 discharge time series data, subsurface flow at the site is routed and or stored through a combination of three pathways. The three flow routing components include the site's upper mineral system composed of silty soils and a clay accumulation horizon, the underlying mineral system made up of clayey soils and the epikarst and lastly a shallow karstic drainage pathway/network originating in the silty-soil horizon. An in depth discussion on the study site's pedology, lithology, karstification, and recharge zone determination has been presented by Meeks and Hunkeler (2015). As demonstrated by Meeks and Hunkeler (2015), shallow vadose zone processes can have a governing role in karst aquifer dynamics, as is the case at the VCB and Areuse Catchment, and that assessment of infiltration in sub-catchments can shine light on aquifer-scale infiltration, storage and drainage patterns. Further the VCB site aligns with DeWalle and Rango (2008) suggested optimal conditions for direct percolation of melt water into the subsurface: negligible slope, lack of soil frost and permeable soils and strata. With these conditions, runoff was insignificant and the balance of melt water was assumed to infiltrate into the soils and groundwater (Mullem et al., 2004).

The VCB receives approximately 1550 mm of precipitation annually, 30–40% of which falls as snow between the months of December and March (www.meteoswiss.ch). A proximal Swiss Agrometeo weather station in Les Verriers (525500, 199175 UPS; Campbell-CR10x) shows that average summer and winter temperatures for the area are +14 °C and −1 °C respectively. The VCB catchment is primarily vegetated by cocksfoot and ryegrass species.

The size of the VCB1 catchment area was identified using a series of isolated summer rain events of varying intensity and duration, as observed in VCB1 hydrograph records (Meeks and Hunkeler, 2015). The integrated area ($m^3$) under each summer-storm event hydrograph was divided by its corresponding total-event precipitation (m), resulting in a recharge area ($m^2$). It should be noted that karst aquifers are known to have time variant recharge areas (Hartmann et al., 2013, 2012). This effect is not considered here. An in-depth discussion on the validity of using a catchment area of 1600 $m^2$, despite the influences of a time-variant catchment size, is presented in Meeks and Hunkeler (2015).

A series of unpublished VCB tracer tests revealed the approximate VCB1 recharge location to be north and adjacent to the cave's orientation. A 1979 tracer test proved hydraulic connection between the VCB cave and the Areuse Spring, the drainage point of the Areuse watershed (Müller et al., 1982). Meeks and Hunkeler (2015) normalized the VCB1 and Areuse Spring discharges to one another according to their respective catchment areas. These normalized discharges agree surprisingly well despite the large difference in catchments size and despite relying on measurements from "opposite ends" of the groundwater flow systems. This hydrograph agreement indicates the relevance of shallow vadose zone processes on karst aquifer dynamics and that the inverse modeling of snowmelt from cave drainage could be extrapolated to the larger watershed scale (Meeks and Hunkeler, 2015).

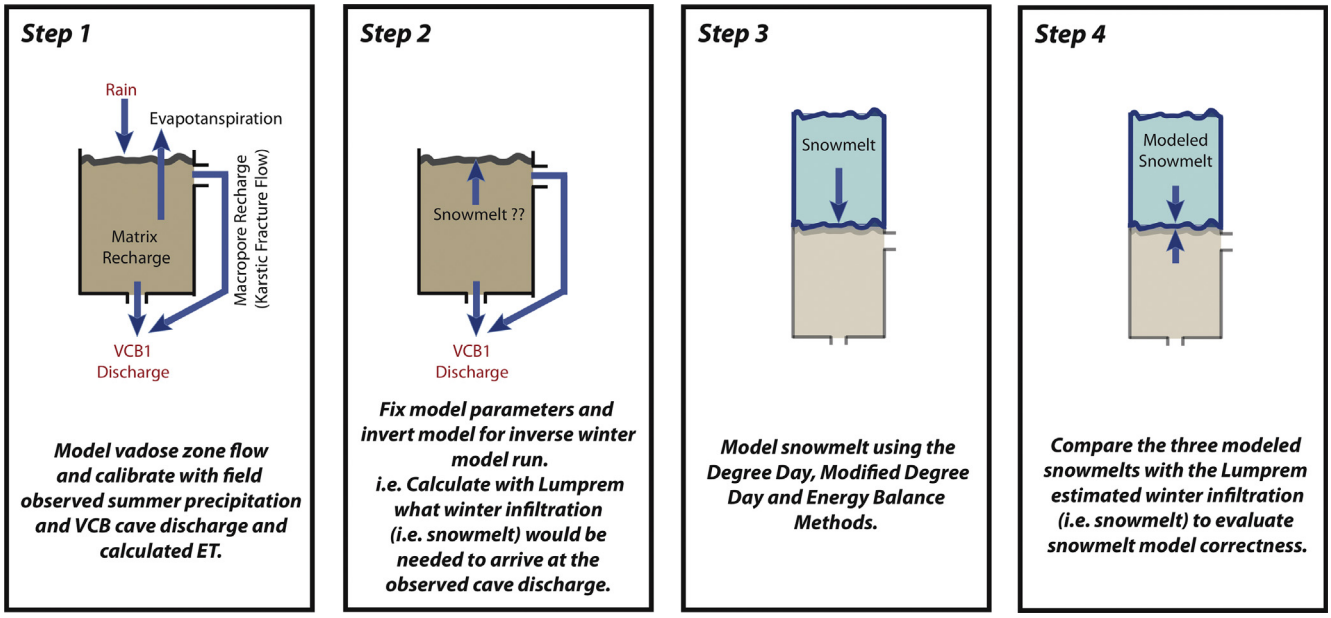


**Fig. 1.** Workflow of the modeling completed using the Vers Chez le Brandt (VCB) calibration data. Each of the four models (Lumprem, degree-day, modified degree-day and energy balance) was subject to a null-space Monte-Carlo calibration.

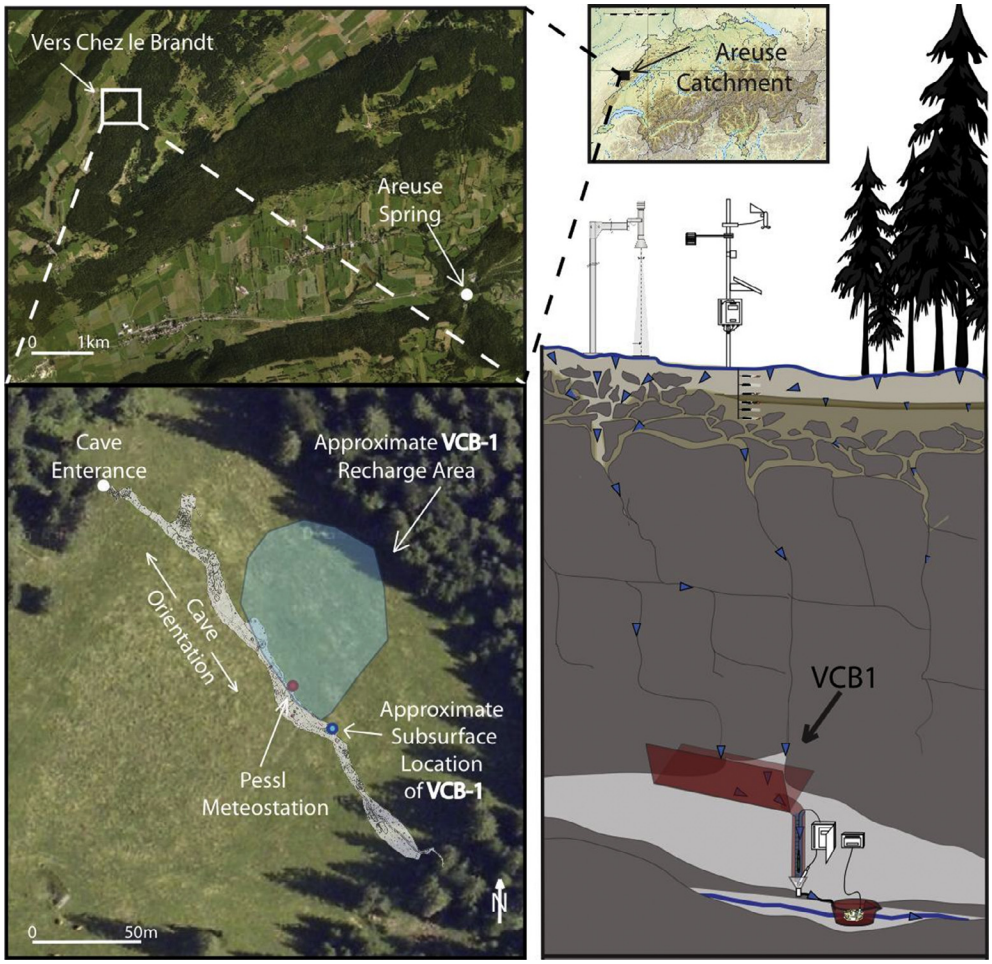


**Fig. 2.** Counterclockwise is the Areuse Catchment location, Vers chez le Brandt (VCB) and Areuse Spring locations, the VCB areal configuration showing the site's underlying cave, and a not-to-scale conceptual model of site cross section with surficial and cave instrumentation.

## 3. Data

Between November 16, 2011 and May 16, 2013, VCB air temperature (range of −40 °C to 60 °C, accuracy of ±0.1 °C), relative humidity (range of 0–100%, accuracy of 1%), global radiation (range of 0–2000 W/m$^2$), wind speed and direction and precipitation were recorded hourly by a Pessl iMETOS Pro meteostation. An attached Sommer USH-8 Ultrasonic Snow-depth sensor (range of 0–8 m, accuracy of ±1 cm) simultaneously measured snow depth. Methylene-blue frost tubes, which extended 30 cm into the VCB soil substrate, did not indicate the presence of soil frost at any point during snow cover. A funneling device mounted to the cave roof, directed VCB1 discharge water to a vertical PVC pipe, within which suspended a pressure transducer measuring water stage. Water stage was then correlated to discharge volume via manual discharge measurements collected weekly throughout the 2010–2013 test period. VCB1 stage was monitored hourly between November 16, 2011 and May 16, 2013 to generate discharge data representing the drainage for the entire VCB catchment. This data was then divided by the recharge area to arrive at point discharge data used in the calibration of the vadose zone model. A detailed depiction of cave instrumentation and overall site configuration can be found in Meeks and Hunkeler (2015). Additionally, weekly snow cores were randomly collected throughout the VCB1 recharge area for later establishment of SWE.

Weekly snow cores were randomly collected throughout the VCB1 recharge area for later establishment of SWE. Manual measurement of SWE, via snow samples collected in snowtubes, served as calibration data for the snowmelt models. While the sampling devices and methods used were "industry standard", immaculately collection of a snow sample is impossible as small amounts of snow were lodged in the uneven and grass-covered ground surface and therefor left unaccounted. More importantly, collected SWE samples may not have reflected the distributed average SWE within the capture zone, as snow packs have a high anisotropy and by very nature snow cores are discreet samples. To overcome this inherent limitation, we collected SWE samples randomly throughout the recharge area and performed a few snow courses to establish the range of SWE values at a given time (on average ∼15 cm). The later exercise was only performed three times throughout the winter, as the capture zone is only 1600 m$^2$ and repeated snow courses would have greatly disturbed the snowpack in the relatively small recharge zone and possible alter infiltration rates.

## 4. Modeling

In the following section, we define the Lumprem model, which serves to generate the dataset of snowmelt infiltration and the point of comparison for the snowmelt models' output. Then we describe the three applied snowmelt models, of varying degrees of mathematical complexity and physical basis, used to simulate snowpack accumulation and ablation and consequent snowpack drainage.

### 4.1. Lumprem

The 1-D unsaturated zone model LUMPREM (LUMPed Parameter REcharge Model) was used to back-calculate infiltration from VCB1 discharge. This semi-physically based, lumped parameter model is capable of providing basic simulation of major unsaturated zone water balance components including rainfall, evapotranspiration, recharge, macro-pore recharge and runoff (Watson et al., 2013). This latter process in the model is turned off for this study given the lack of observed runoff at the VCB site. Lumprem serves as the user and data interface to the subroutine RECHMOD (RECHarge MODel), where all model calculations pertaining to water movement and storage within the vadose zone take place. The model receives field-measured precipitation (cm) and calculated evapotranspiration (cm, ETo) as hourly inputs. Daily ETo was calculated using the FAO56 Penman-Monteith method (Allen and Pruitt, 1991). Input data for ETo calculations included field-measured average solar radiation, minimum and maximum air temperature, minimum and maximum relative humidity, dew point and wind speed for each day. Given that the evapotranspiration rate of plants is dependent on the volume of available water in the unsaturated zone, water loss through evapotranspiration was calculated in Lumprem using the following equation:

$$E = fE_p \frac{1 - e^{-\gamma v'}}{1 - 2e^{-\gamma} + e^{-\gamma v'}} \quad (1)$$

where $E$ is water loss through evapotranspiration, $E_p$ is potential evapotranspiration (ETo is used in exchange for $E_p$ within this model), $f$ is a crop factor, $v'$ is the relative volume of water in the container (ie. $V/V_{max}$ where V is the current amount of water in the container and $V_{max}$ is the total container volume), and $\gamma$ is a parameter determining the shape of the evapotranspiration rate versus the stored water relationship.

Recharge, as calculated by Lumprem, is the water lost from the model bucket as a continuous unsaturated vertical flow to the subsurface underlying the root zone. Since hydraulic conductivity of unsaturated material decreases with decreasing saturation, the rate at which water is lost from the bucket depends on the volume of moisture currently stored. In accordance with van Genuchten's (1980) equation, rate of water lost as recharge is expressed by the following equation:

$$R = K_s [v']^l \left[1 - \left(1 - [v']^{l/m}\right)^m\right]^2 \quad (2)$$

where $R$ is rate of drainage, $K_s$ is saturated hydraulic conductivity, $l$ is the pore-connectivity parameter (estimated by Mualem (1976) to be about 0.5 for many soils), and $m$ is a parameter determining the shape of the drainage rate versus stored water relationship.

Macro-pore recharge ($R_m$), a phenomena quite common in karstic aquifers, occurs when temporary saturated conditions in the upper subsurface allow water to migrate laterally to zones of preferential downward flow. Lumprem allows for this type of drainage when saturated conditions occur in the soil store. Given that runoff is not present in this system, all overflow of the bucket become macro-pore recharge.

### 4.2. Degree-day snowmelt model

SWE evolution was simulated based on the melt equations governing HBV's (Bergstrom and Singh, 1995; Sten, 1975) snow routine.

$$M = \left(\frac{C}{24}\right) * (T_a - T_t) \quad (3)$$

where M is melt ($mm\,h^{-1}$), C is the degree-day factor ($mm\,°C^{-1}\,h^{-1}$), $T_a$ is the mean hourly air temperature (°C), and $T_t$ is the threshold temperature (°C). The model accounts for the inputs and outputs for both the liquid and solid stores along with water retention capacity of the snowpack and refreezing of meltwater.

$$R = C_{fr} * C(T_t - T_a) \quad (4)$$

where R is refreezing ($mm\,h^{-1}$) and $C_{fr}$ is the refreezing coefficient, the latter of which assumed a default value of 0.05. Measured hourly precipitation and temperature served as input parameters, while hourly snowpack drainage was model output.

The degree-day model can have limited ability to appropriately assessing sub-daily time increments due to the variations in the correlation between air temperature and snowpack energy supply between day and night periods (DeWalle and Rango, 2008). That withstanding, hourly simulations were completed in this study to: 1. provide a more accurate comparison to the physically based model, which is capable of accurate hourly melt simulation; and 2. to stay consistent with the high reactivity of the vadose zone to recharging water, where infiltrating waters transit the unsaturated zone in under an hour. Further, the daily aggregate of hourly simulations, rendered the same simulation results as discussed below, just in a courser time step.

All three snow process models use a constant but calibrated threshold temperature at which rain converts to snow or vice versa. In reality, a temperature range exists in which the percentage of rain decreases as the percentage of fallen snow increases, when air temperature cools.

In total, the degree-day model has three parameters, which have to be calculated ($T_t$, C, and SCF, the latter a snowfall correction factor) and two time series inputs ($T_a$ and precipitation).

### 4.3. Modified degree-day snowmelt model

While many adaptations to the degree-day approach (Brubaker et al., 1996; Cazorzi and Dalla Fontana, 1996; Hock, 2003; Kuusisto, 1980; Pellicciotti et al., 2005) have been fabricated to overcome the model's simplicity and consequent limitations, the recently developed Tobin method (Tobin et al., 2013) was selected as a midpoint in assessed model complexity (i.e. physical basis). The Tobin method uses measured daily air temperature extremes to impose a diurnal cycle on the melt rate. The resulting time variant degree factor ($A_s$) accounts for the actual distribution of snowmelt rates in time, which peak at hours of maximum incident radiation and fall to a minimum during the night (Tobin et al., 2013). The association between C and $A_s$ is as follows:

$$A_s = \begin{cases} C + \beta\Delta_T \sin\left(\pi \frac{t_d - t_o}{t_1 - t_0}\right) & t_0 \leqslant t_d < t_1 \\ C - \beta\Delta_T Z & otherwise \end{cases} \quad (5)$$

where $\beta$ is a factor to convert the temperature amplitude into a degree-day factor amplitude, $\Delta_T$ is the difference between the maximum and the minimum daily temperature on day $d$ (h), $t_d$ is the hour of the day $d$ (h), $t_0$ is the start time of daylight on day $d$, $t_1$ is the end time of daylight on day $d$ and Z is a factor to ensure that the daily mean value of $A_s$ equals C.

$$Z = 2\frac{t_1 - t_o}{\pi l_n} \quad (6)$$

where $l_n$ (h) is the duration of the night.

$$l_n = 24 - t_1 + t_o \quad (7)$$

Similarly to the classic degree-day method, the Tobin approach accounts for the solid (snow) and liquid (rain) water inputs to the system and the solid and liquid water content of the snowpack (refreezing and drainage). Snowpack drainage incorporates both rain and melting snow.

The modified degree-day model had four parameters that have to be calibrated ($T_t$, C, SCF, and $\beta$) and five time series inputs ($T_a$, $t_1$, $t_0$, $\Delta_T$ and precipitation).

### 4.4. Energy balance snowmelt model

The point energy balance model used to simulate the energy and mass balance and melt rates of the VCB's snow surface was based on melt equations of ESCIMO.spread (Strasser and Marke, 2010). The 1-D, single-layer process model considers short and long wave radiation, sensible and latent heat fluxes, energy conducted by solid and liquid precipitation as well as sublimation/re-sublimation and a constant soil heat flux. This physically based model assumes a homogeneous, isotropic snowpack and does not consider lateral process in the mass balance calculation. For snowmelt to occur, a snow cover must be present at a given time step and the surface energy balance must be positive, indicating that energy is available for snowmelt. In keeping with ESCIMO.spread, the used energy balance model had eight parameters that required calibration ($A_{min}$, $A_{add}$, $DP_p$, $DP_n$, SS, $S_e$, SHF, and $T_p$). Input included VCB field measured air temperature (K), relative humidity (%), wind speed (m/s), precipitation (mm $h^{-1}$) and global radiation ($W/m^2$) along with calculated incoming longwave radiation ($Q_{l\downarrow}$, $W/m^2$). This latter parameter was derived using the Stefan-Boltzmann constant:

$$Q_{l\downarrow} = \sigma \cdot \varepsilon \cdot T_a^4 \tag{8}$$

where $T_a$ is the air temperature (K) at 2 m and $\varepsilon$ is atmospheric emissivity. This latter parameter was established using Prata's (1996) approach:

$$\varepsilon = 1 - (1 + W_p) \cdot e^{-(1.2+3W_p)^{0.5}} \tag{9}$$

$W_p$ is the precipitable water as an empirical function of actual vapor pressure and air temperature.

$$W_p = 46.5 \cdot \frac{e_o}{T_a} \tag{10}$$

where $e_o$ is the actual vapor pressure (kPa) and was calculated in following with the FAO56 method (Allen et al., 1998).

## 5. Calibration

All four models were calibrated using the automatic parameter estimation software PEST (Doherty et al., 2016). The suitable parameters sets were found using a null space Monte Carlo (NSMC) approach, wherein 10,000 random parameter values were generated. NSMC allows the computational demand of a standard Monte-Carlo approach. NSMC is readily available through two powerful tools of the PEST-suite, SVD-assist (Tonkin and Doherty, 2005) and pre-calibration null space projection (Doherty and Hunt, 2009). In the former, parameter space was subdivided into solution and null spaces. The subdivision took place only once and the number of estimated parameters was equal to the number of chosen dimensions of the solution space. The latter PEST tool was used to modify random parameter sets in the null space (NSMC). A variation of a parameter in the null space will not affect the target objective function (OF), defined in this study as 6000 $mm^2$, wherein the squared difference between the observed and calculated snow water equivalent was minimized.

Through this calibration approach, it was possible to efficiently obtain a set of very different parameter fields, which respect both the stochastic variability of the model parameters as well as the historical measurements of system state with only a handful of runs per parameter field (Moeck et al., 2015). For more details the interested reader is refereed to (Dausman et al., 2010; Doherty, 2003; Fienen et al., 2009; Tonkin and Doherty, 2009).

### 5.1. Lumprem

Lumprem calibration occurred in two phases. In the initial phase, herein referred to as the "forward" Lumprem calibration, model parameters for soil and vegetation were calibrated based on observed hourly precipitation (rain) and VCB1 discharge for the snow-free period (04/01/12 00:00–6/22/2012 23:00) following the above detailed process. The initial 311 h (until 4/13/2012 23:00) served as a model warm up phase to consider antecedent soil moisture prior to the calibration of the modeled vadose zone system. Following the calibration, the period between 6/23/2012 00:00 and 11/21/2012 23:00 was used to validate the calibration. The best-estimated parameter set for Lumprem's forward calibration had the smallest differences between observed and simulated discharge (mean-error for the test period) for the calibration and validation period.

In Lumprem's second phase of use, herein referred to as the "inverse" Lumprem calibration, the model was fixed using the 30 best-estimated parameter sets from the forward Lumprem calibration. Lumprem was then used to estimate the amount of snowmelt infiltration needed to arrive at the observed VCB1 discharge, between the winter period of 11/1/12 00:00 and 6/1/13 00:00. Lumprem's 30 inverse optimizations are presented in the results and discussion as the point of comparison for the snow process models' output.

### 5.2. Snowmelt models

The degree-day, modified degree-day and energy balance snow process models were calibrated to manual SWE measurements for the period between 11/1/12 00:00 and 6/1/13 00:00 following the above detailed process. SWE values were log transferred and given equal weights during the PEST calibration. We assumed that all observations are equally relevant and therefore the weights are not changing between the observations. We calibrated $T_t$, C, and SCF for the degree-day model, $T_t$, C, SCF, and $\beta$ for the modified degree-day model, and $A_{min}$, $A_{add}$, $DP_p$, $DP_n$, SS, $S_e$, SHF, and $T_p$ for the energy balance model. Success of snow process simulation (for the best-fit parameter set for each snowmelt model) was evaluated via coefficient of determination ($R^2$), index of agreement (IA), (Willmott, 1981) and Nash-Sutcliffe model efficiency (NSME), (Nash and Sutcliffe, 1970).

## 6. Results

Degree of snow process model success was defined by the models' ability to meet the objective function of 6000 $mm^2$. One iteration of the modified degree-day, 15 iterations of the energy balance and none of the classic degree-day iterations met the objective function. Given this range of ability to meet the OF, snow model results are compared in two ways; firstly according to the 30 best-fit iterations for each respective model; and secondly according to the iterations that actually met the objective function.

Over all, Lumprem was able to reproduce observed VCB1 discharge during the summer forward calibration and validation periods very well (the time series of observed VCB1 discharge and Lumprem estimated discharge, using the optimal parameter set for the forward calibration and validation are presented in Fig. 3). However, the validation period underestimated peak discharge events and was not able to fit the tailing of individual hydrograph events with great accuracy. During the validation phase, peak discharge was overestimated by Lumprem and

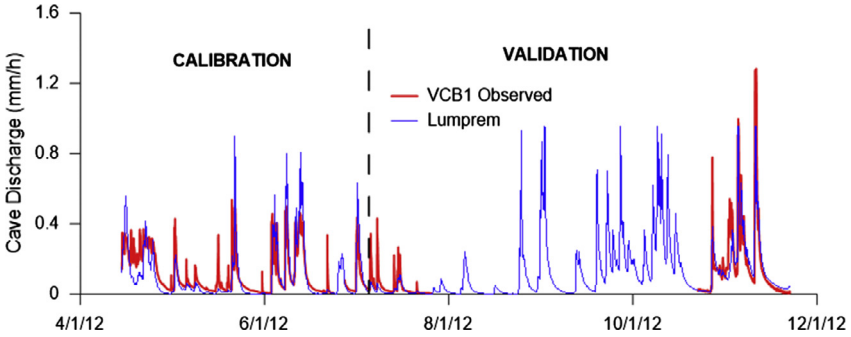


**Fig. 3.** Best-fit Lumprem calibration and validation during snow-free summer and fall.

modeled event hydrograph recessions more closely matched observed decreases in flow within the cave. The gap in observed VCB1 discharge resulted from equipment failure in the cave. Lumprem inversely estimated a total accumulated infiltration from snowmelt to have been between 493 and 837 mm, with the mean cumulative infiltration of 703 mm. Fig. 4 shows the cumulative, inversely-estimated snowpack drainage from Lumprem (30 best-fit iterations and ensemble mean (EM, the average of the model results from the 30 best-fit parameter sets)) along with the simulated cumulative drainage by the snowmelt models. Only the iterations that met the objective function are presented for the modified degree-day and the energy balance models. In contrast, the 30 best-fit iterations for the classic degree-day (none of which met the objective function) are presented in this figure. Increases in cumulative Lumprem modeled infiltration correspond with either rain (or mixed precipitation) on snow events (end of December, beginning of February and April) or positive air temperatures (mid March). Periods of snow accrual with consistently negative air temperatures (second half of February) did not correlate to an inversely modeled increase in snowmelt infiltration.

The classic degree-day method over estimated the early-winter snow accumulation in December, underestimated snow accumulation in January, and initially underestimated and then overestimated SWE during the melt phase in March and April. None of the classic degree-day iterations reached the objective function of 6000 $mm^2$. The range in cumulative drainage from the snowpack is relatively small, between 518 and 638 mm, and lies in the lower bounds of the range of inversely estimated snowpack drainage from Lumprem (493–837 mm). The EM for degree-day simulation of snowpack drainage is approximately 110 mm less than the ensemble mean generated by Lumprem. A boxplot of the calibrated parameters representing the 30 best-fit NSMC simulations is presented in Fig. 5. The model's SCF maintained the highest parameter variability while the C maintained the least. This calibration resulted in a NSME of 0.16, a $R^2$ of 0.31 and an IA of 0.75.

While able to reproduce SWE values, on average, the modified degree-day modeling approach slightly overestimated SWE during the accumulation phase of early winter and then slightly underestimated SWE during the slow accumulation phase in January (Fig. 6). The modified degree-day approach then went on to initially underestimate and then overestimate SWE during the spring snowmelt phase. When considering the 30 best-fit iterations, the modified degree-day model had a larger variability of estimated cumulative snowpack drainage, ranging between 448 and 650 mm, with an ensemble mean of 524 mm, approximately 167 mm less than what was estimated by Lumprem (EM). Of these 30 iterations, only one was able to achieve the objective function, which presented a cumulative drainage of 458.4 mm. This iteration had a C of 1.1, a SCF of 0.73, a $T_t$ of 2.7, and a $\beta$ of 0.96 and resulted in a NSME of 0.72, a $R^2$ of 0.73 and IA of 0.92. Similarly to its more simplified cousin, the model's SCF maintained the highest parameter variability while the C maintained the least. However, with the introduction of the temperature amplitude conversion factor, the three calibrated parameters that were also used in the classic degree-day approach had an increase in parameter variability of approximately 100% in relation to that observed in the simplified degree-day version.

The energy balance model reproduced observed SWE measurements very well throughout the entire winter, with only nominal underestimates of mid-winter observations (Fig. 6). The cumulative snowpack drainage, as indicated by the EM, was only 49 mm less than that estimated by Lumprem (EM) and presented a potential cumulative range of 625 and 656 mm. 15 iterations reached the objective function with the calibrated parameters ranging accordingly: $A_{min}$ (0.57–0.6), $A_{add}$ (0.35–0.45), $DP_p$ (0.05–1), $DP_n$ (0.02–0.06), SS (0.18–1.91), $S_e$ (0.7–0.78), SHF (1–3), and $T_p$ (272.16–276.16). The cumulative drainage for these 15 iterations ranged between 653 mm and 662 mm (Fig. 4). The iteration with the lowest objective function presented a cumulative drainage of 656 mm (only 40 mm less than that estimated by Lumprem (EM)) and resulted in an IA of 0.98, a $R^2$ of 0.91 and a NSME of 0.91. Albedo ($A_{min}$ and $A_{add}$), decline parameter (positive temperatures) and snow emissivity presented the highest parameter variability while soil heat flux and phase transition temperature presented the lowest (Fig. 5).

## 7. Discussion

This is the first study to systematically compare the uncertainties surrounding modeled predictions for recharge from snowmelt. It is important to distinguish the contributing sources of uncertainty. The first category resulted from the input data used to calibrate the models, while the second category resulted from the modeling approaches themselves. While snow process model predictions are the aim of this study, we will begin the discussion by evaluating the uncertainty arising from the models' input.

As depicted in Fig. 4, cumulative snowpack drainage estimated by the snowmelt models and Lumprem do not coincide perfectly, principally so in the first half of the winter. During this time, Lumprem simulated two infiltration events (12/15/12–12/27/14 and 1/28/13–2/4/13) that were only marginally detected by the three snowmelt models. The synchronous underestimation of snowpack drainage in the first half of winter by all three snowmelt models, which range between physically based and index, implies input data error. In the first half of winter, precipitation data was derived from an insulated and heated tipping bucket attached to the remotely-located weather station. A solar panel sourced electricity to the tipping bucket's heating unit. The small heating unit, limited by its electrical supply, was unable to generate enough heat to melt

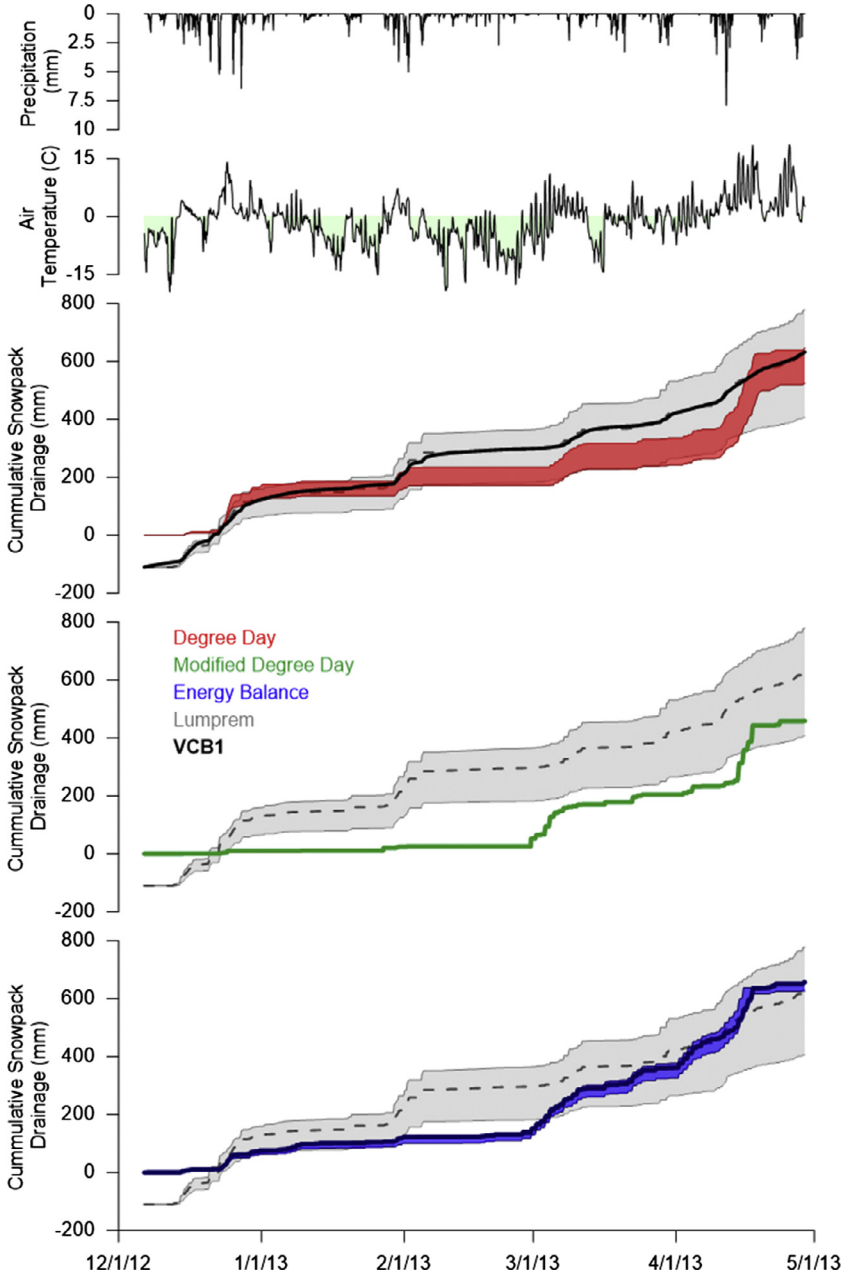


**Fig. 4.** Comparison of accumulative snowpack drainage for each snowmelt model with Lumprem's inversely estimated snowpack drainage. Depicted are the; thirty best-fit Lumprem iterations for inversely estimated snowmelt (gray); the ensemble mean of the thirty best-fit Lumprem iterations (dashed line); the discharge observed at the VCB (black line overlying the degree-day plot); the thirty best-fit degree-day iterations (none having met the objective function, red); the one modified degree-day iteration that met the objective function (green); the 15 energy balance iterations that met the objective function (blue); and the energy balance iteration with the lowest objective function (black line overlying energy balance plot). Lumprem results are offset by 110 mm to account for a melt event at the beginning of winter that was not observed by the snow models. (For interpretation of the references to color in this figure legend, the reader is referred to the web version of this article.)

all fallen snow and prevent ice bridging. Therefor on 2/22/13, a more rigorous precipitation gauge was installed approximately 3 km away at the closest source of electricity. An increased electrical supply allowed for a more robust heating unit in a larger weighting precipitation gauge. Snow bridging was never observed at this latter instrument. The weighting precipitation gauge was not installed earlier due to lack of observed snow bridging in the previous winter and a consequent lack of knowledge of the need for a hardier device. As a reminder, Lumprem's inversely estimated infiltration during the winter is based solely on discharge observed in the cave. Therefor, the two early-winter infiltration events are believed to be "real" as they are not biased by concurrent precipitation measurements. The lack of observed snowpack drainage by all three models during these two periods implicates precipitation under-catch by the original tipping bucket as the source of off-set shown in the cumulative plots of Fig. 4. Tipping bucket gauge under-catch relative to weighting gauges, particularity during periods of snowfall has been estimated to be upwards of 22% (Hanson et al., 1999). Furthermore, Gurtz et al. (2003) showed that liquid and solid precipitation measurements with conventional gauge are associated with large errors. They applied time depending monthly correction factors which were high in late fall, over the entire winter and early spring, starting from +5% in October for rainfall and rising up to +62% in March for snow. The discrepancy

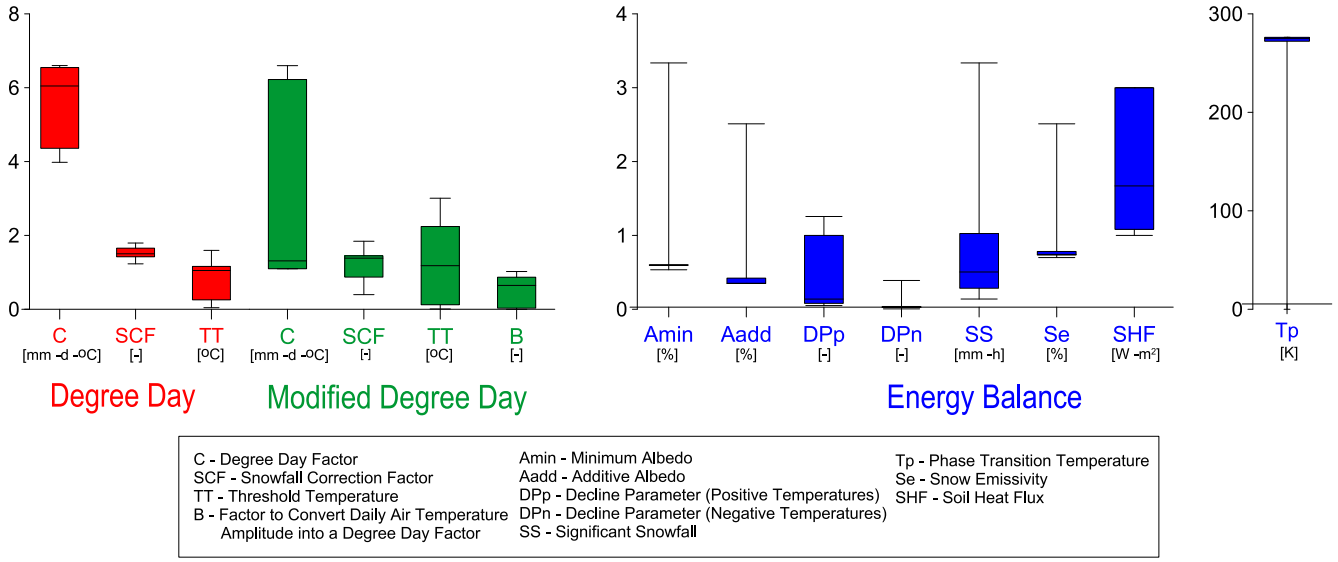


**Fig. 5.** Boxplot of calibrated parameters representing the 30 best-fit NSMC simulations for each of the three snowmelt models.

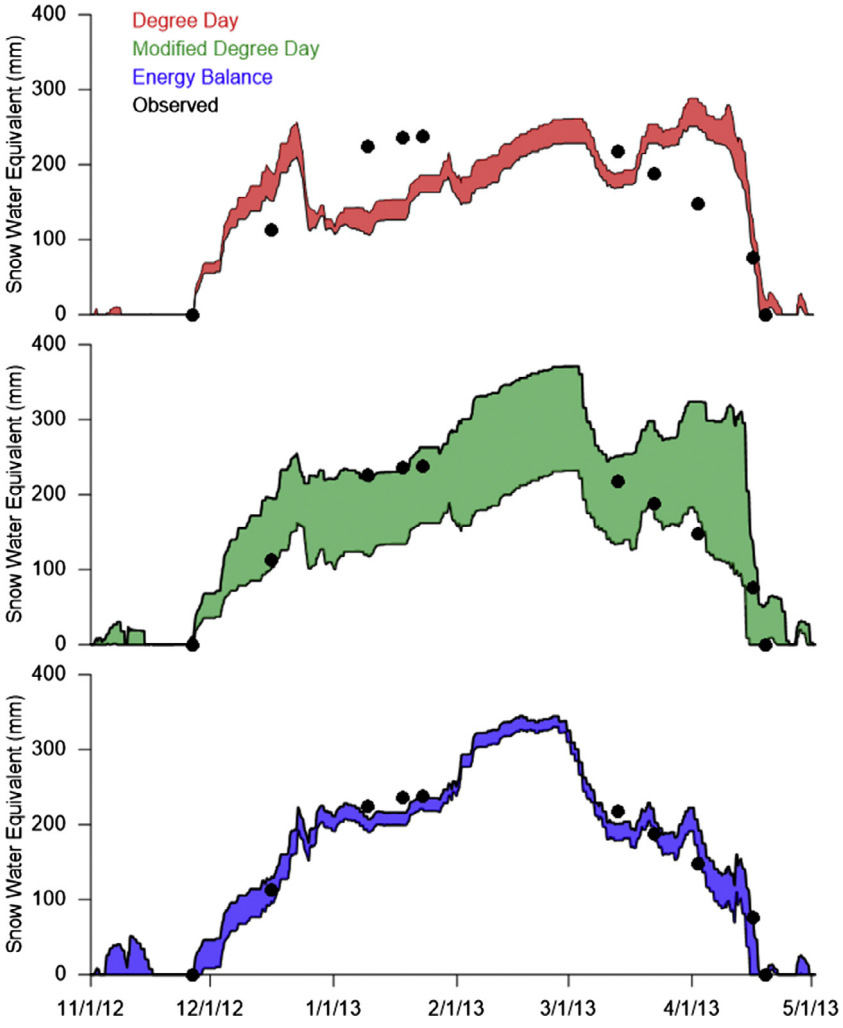


**Fig. 6.** Shows the range of the 30 best-fit null-space Monte Carlo iterations for each snowmelt model. The black dots represent the field-measured SWE.

between the snowmelt models and Lumprem in the first half of winter re-affirms that selection of precipitation measurement device is absolutely paramount in snowmelt modeling studies.

The second source of uncertainty, and principal motivation for this study, resides in the snow process models' structural ability to predict loss of SWE, i.e. available infiltration for recharge. Lower reproducibility of SWE by the index model is logical, given that physical properties such as vapor pressure, albedo, and wind are known to influence the energy balance and snowmelt processes (Tobin et al., 2013) and are not explicitly accounted for. The elevated parameter variability for the degree-day factor (C, Fig. 5) relative to the other variable, most likely resulted from air temperature serving as a proxy for the all the physical forces acting on and within snowpack.

The modified degree-day model was able to more closely approximate the accumulation and ablation of VCB SWE, however only using certain parameter sets resulting from the calibration. This modified index method used a factor (β) to account for the semi-sinusoidal fluctuations in daily air temperature, which indirectly accounts for environmental aspects like cloud cover, length of day, and seasonality. The robustness of this approach is called into question though, when considering the doubling of parameter variability for the degree-day factor, snowfall correction factor and the threshold temperature that arises with the addition of $\beta$ in the calibration. While parameter variability is significantly greater than in the degree-day approach, the model does allow for the opportunity to more closely reproduce observed SWE data, emphasizing the importance of a NSMC simulation coupled with parameter estimation software in modified index models.

The energy balance model presented the smallest snowpack drainage range of the three models when considering the 30 best-fit iterations, with the 15 best-fit NSMC runs resulting in only mild deviations of modeled accumulation and ablation (Fig. 4). As the energy balance equations used in this study were in keeping with those of ESCIMO.spread, latent and sensible heat fluxes, sublimation and re-sublimation, snow age and albedo and the constancy of soil heat flux may serve as sources of model error (Strasser and Marke, 2010). For example, parameter variability may have developed from the simplified calculation of turbulent fluxes, which assumes a medium snow surface roughness and stable snow-surface temperature. In areas where the contribution of the turbulent fluxes to the energy balance of the snowpack is small, the induced loss of model accuracy is negligible (Strasser and Marke, 2010), however stable conditions never truly exist and snow roughness certainly varied throughout the winter. Also, in our model, advective energy supplied by precipitation depends on its phase. Since the percentage of precipitation attributed to each phase was not measured, an adjustable threshold temperature was assumed for the distinction between snow and rain, thereby inducing potential error into the advective component of the energy balance equation. As noted, this latter source of error resulting from a course consideration of the rain/snow phase transition, was uniform throughout all the snowmelt models. All models used the same amount of precipitation in the same form at a given time. Given this consistency across models, this source of uncertainty is not overly important in this study, as the induced uncertainty would be consistent across all snow models. More precise energy balance assessment of accumulation and melt parameters is possible, such as surface roughness, wind speed and snow surface temperature, but with the added cost of high precision instrumentation that was beyond the scope of this study.

While the NSMC parameter sets used for Lumprem's calibration resulted in a large variability of cumulative infiltration (383–727 mm, Fig. 4) at the end of the snow period, the ensemble mean of the 30 best-fit iterations overlies almost perfectly with the cumulative discharge from VCB1 within the cave. This implies Lumprem's successful performance at inverse estimation of snowpack drainage and also reveals that ensemble means should be applied to produce credible predictions of snow drainage and the associated uncertainties. If only one realization of Lumprem, and each snowmelt model, had been completed, our results and associated conclusions would have been greatly altered. As depicted in Fig. 4, all three snowmelt models underestimate cumulative snowpack drainage. When considering the potential precipitation under-catch of 22% in the first part of winter, the degree-day model would have underestimated (based on the EM) cumulative snowpack drainage by 65 mm; the modified degree-day model would have underestimated (based on the iteration with the lowest objective function) drainage by 215 mm; and the energy balance would have underestimated (based on the iteration with the lowest objective function) drainage by 14 mm when compared to the Lumprem's estimated cumulative drainage (EM). These underestimates respectively account for 9%, 31% or 2% of the total Lumprem estimated (EM) drainage by the end of the snow period.

When comparing the trends in cumulative increases in snowpack drainage over time (EM for each model), some interesting observations can be made. With increased complexity of snowmelt model, there is an increased underestimation of snowpack drainage during the first half of winter. While the underestimation of snowmelt rates in the early part of the snow season is probably related to input error associated with precipitation under-catch, this error is consistent across all models. Through the second half of winter, the degree-day model initially tracks Lumprem drainage well, but then grossly overestimated rate of snowpack drainage. This latter period speaks of the degree-day model's oversensitivity to air temperature. The modified degree-day model tracks similarly to the classic degree-day approach. The energy balance model maintains a more persistent overestimation throughout the second half of winter, issuing to the models more parametrically distributed sources of uncertainty tying into the computation of latent and sensible heat fluxes, sublimation and re-sublimation, snow age and albedo.

The finding from this study must be considered in light of how snow process models are typically used. Water management agencies may apply snow process models to understand such things as melt pulses resulting from a rain on snow events (as might be the case for flood protection or water quality monitoring), or to determine a snowmelt's contribution to an annual water budget (such as contributions of snowmelt to base flow in the summer). The results show that none of our models are well suited for very short time scales, but rather the longer seasonal scale. Our study reinforces the need to carefully choose the model based on not only in terms of uncertainty surrounding predications but also temporal scale associated with intended application of model results.

Overall, the results indicate that with increased physical basis to the model and increased parameterization of the factors influencing melt and accumulation, there is a higher ability of the model to reproduce the observed SWE values. Further these results show that will rigorous calibration, one can achieve model results that have low uncertainty surrounding predictions and produce results that are within the realm of reality as is the case for the energy balance model.

## 8. Conclusions

As water demands outstrip water supply, more in depth knowledge of recharge processes will be needed. The rate and timing of infiltration from snowmelt is frequently devised via snowmelt models, with varying degrees of complexity and physical basis. Given the importance of snow process model results for water

management agencies, we presented here the results from the first systematic inter-comparison of uncertainties associated with modeled snowmelt predictions. Back-calculated snowmelt data was used as a point of comparison for three snowmelt algorithms; a simple degree-day model, a modified degree-day model and an energy balance snowmelt model. Through null space Monte Carlo calibration, we evaluated the performance and uncertainty arising from each snowmelt model's predictions. When compared with the back-calculated snowmelt, all three melt models underestimate total snowpack drainage, underestimate the rate of early and midwinter drainage (possibly related to precipitation gauge under-catch) and overestimate spring snowmelt rates. Further, the rate of snowpack water loss is more constant over the course of the entire winter season than the snowmelt models would imply when compared to the back-calculated snowmelt. These results indicate that mid-winter melt can contribute as significantly as springtime snowmelt to groundwater recharge. Further, these groundwater management agencies bodies should be aware that actual groundwater renewal could be between 2 and 31% greater than snowmelt models suggest.

The choice of the snowmelt model used might be dictated by the available data. For example, in many cases only temperature data is available and thus only the day-degree method can be use. Our study however shows that the uncertainties are considerable for snowmelt modeling and can be reduced by inclusion of more data that is integrated into a more complex approach such as the energy balance method, and that in any case quantifying the uncertainties should be done. This study demonstrated that an uncertainty analysis of model predictions is easily accomplished due to the low computational demand of the models and efficient calibration software. Further, this analysis is absolutely worth the additional investment as it allows model users to arrive at an optimal model realization with a minimized objective function.

Also, this study was only possible due to the solid data for the infiltration under the snowpack, generated via the unique, oversized, natural lysimeter of our field site. The importance of real distributed calibration data such as this cannot be underestimated or understated. Given that the geology allowing for a study such as this is quite uncommon, development of a systematic instrumentation that evaluates the distributed, temporal evolution of snowpack drainage is paramount for optimal understanding and management of cold-climate hydrologic systems.

## References


Allen, R., Pruitt, W., 1991. FAO-24 reference evapotranspiration factors. J. Irrigation Drainage Eng. 117 (5), 758–773.

Allen, R.G., Pereira, L., Raes, D., Smith, M., 1998. FAO Irrigation and Drainage Paper No. 56. Food and Agriculture Organization of the United Nations, Rome, pp. 26–40.

Anderson, E.A., 1968. Development and testing of snow pack energy balance equations. Water Resour. Res. 4 (1), 19–37.

Archer, D., Stewart, D., 1995. The installation and use of a snow pillow to monitor snow water equivalent. Water Environ. J. 9 (3), 221–230.

Bergstrom, S., Singh, V., 1995. The HBV model. In: Computer Models of Watershed Hydrology. pp. 443–476.

Beven, K., Binley, A., 1992. The future of distributed models: model calibration and uncertainty prediction. Hydrol. Process. 6 (3), 279–298.

Brubaker, K., Rango, A., Kustas, W., 1996. Incorporating radiation inputs into the snowmelt runoff model. Hydrol. Process. 10 (10), 1329–1343.

Butcher, P., McManamon, A., 2011. Optimization of a snow observation network via principal component analysis. Proceedings AGU Fall Meeting Abstracts 2011, vol. 1, p. 1305.

Cazorzi, F., Dalla Fontana, G., 1996. Snowmelt modelling by combining air temperature and a distributed radiation index. J. Hydrol. 181 (1), 169–187.

Cline, D., 1995. Snow surface energy exchanges and snownielt at a continental alpine site.

Dausman, A.M., Doherty, J., Langevin, C.D., Sukop, M.C., 2010. Quantifying data worth toward reducing predictive uncertainty. Ground Water 48 (5), 729–740.

DeWalle, D.R., Rango, A., 2008. Principles of Snow Hydrology. Cambridge University Press, Cambridge.

Doherty, J., 2003. Ground water model calibration using pilot points and regularization. Ground Water 41 (2), 170–177.

Doherty, J., Brebber, L., Whyte, P., 2016. PEST: Model-Independent Parameter Estimation, vol. 122. Watermark Computing, Corinda, Australia.

Doherty, J., Hunt, R.J., 2009. Two statistics for evaluating parameter identifiability and error reduction. J. Hydrol. 366 (1), 119–127.

Elouardi, N., 1998. Modèle conceptuel pour la classification des zones épikarstiques en fonction de leurs réponses géophysiques et de leurs propriétés hydrauliques. Exemple du site de Vers Chez le Brandt (NE). Master: University of Neuchatel, 62p.

Etchevers, P., Martin, E., Brown, R., Fierz, C., Lejeune, Y., Bazile, E., Boone, A., Dai, Y.-J., Essery, R., Fernandez, A., 2004. Validation of the energy budget of an alpine snowpack simulated by several snow models (SnowMIP project). Ann. Glaciol. 38 (1), 150–158.

Feng, X., Sahoo, A., Arsenault, K., Houser, P., Luo, Y., Troy, T.J., 2008. The impact of snow model complexity at three CLPX sites. J. Hydrometeorol. 9 (6), 1464–1481.

Fienen, M.N., Muffels, C.T., Hunt, R.J., 2009. On constraining pilot point calibration with regularization in PEST: ground water 47 (6), 835–844.

Franz, K.J., Butcher, P., Ajami, N.K., 2010. Addressing snow model uncertainty for hydrologic prediction. Adv. Water Resour. 33 (8), 820–832.

Gallagher, M., Doherty, J., 2007. Parameter estimation and uncertainty analysis for a watershed model. Environ. Model. Softw. 22 (7), 1000–1020.

Gurtz, J., Verbunt, M., Zappa, M., Moesch, M., Pos, F., Moser, U., 2003. Long-term hydrometeorological measurements and model-based analyses in the hydrological research catchment Rietholzbach. J. Hydrol. Hydromech. 51 (3), 162–174.

Hanson, C.L., Johnson, G.L., Rango, A., 1999. Comparison of precipitation catch between nine measuring systems. J. Hydrol. Eng. 4 (1), 70–76.

Hartmann, A., Barberá, J.A., Lange, J., Andreo, B., Weiler, M., 2013. Progress in the hydrologic simulation of time variant recharge areas of karst systems. Exemplified at a karst spring in Southern Spain. Adv. Water Resour. 54, 149–160.

Hartmann, A., Lange, J., Weiler, M., Arbel, Y., Greenbaum, N., 2012. A new approach to model the spatial and temporal variability of recharge to karst aquifers. Hydrol. Earth Syst. Sci. 16, 2219–2231.

Haupt, H.F., 1969. A 2-year evaluation of the snowmelt lysimeter.

Havlicek, E., 1999. Les Sols Des Paturages Boises du Jura Suisse Master Thesis. University of Neuchatel, p. 212 p.

Herrero, J., Polo, M., Moñino, A., Losada, M., 2009. An energy balance snowmelt model in a Mediterranean site. J. Hydrol. 371 (1), 98–107.

Hock, R., 1999. A distributed temperature-index ice-and snowmelt model including potential direct solar radiation. J. Glaciol. 45 (149), 101–111.

Hock, R., 2003. Temperature index melt modelling in mountain areas. J. Hydrol. 282 (1), 104–115. Äì4.

Hodgkins, R., Carr, S., Pálsson, F., Guðmundsson, S., Björnsson, H., 2012. Sensitivity analysis of temperature-index melt simulations to near-surface lapse rates and degree-day factors at Vestari-Hagafellsjökull, Langjökull, Iceland. Hydrol. Process. 26 (24), 3736–3748.

Jost, G., Dan Moore, R., Smith, R., Gluns, D.R., 2012. Distributed temperature-index snowmelt modelling for forested catchments. J. Hydrol. 420, 87–101.

Kattelmann, R., 1989. Spatial variability of snow-pack outflow at a site in Sierra Nevada, USA. Ann. Glaciol. 13, 124–128.

Kattelmann, R., 2000. Snowmelt lysimeters in the evaluation of snowmelt models. Ann. Glaciol. 31 (1), 406–410.

Kuusisto, E., 1980. On the values and variability of degree-day melting factor in Finland. Hydrol. Res. 11 (5), 235–242.

Linsley, R.K.J., 1943. A simple procedure for the day-to-day forecasting of runoff from snow-melt. Trans. Am. Geophys. Union 24, 62–67.

Magnusson, J., Farinotti, D., Jonas, T., Bavay, M., 2011. Quantitative evaluation of different hydrological modelling approaches in a partly glacierized Swiss watershed. Hydrol. Process. 25 (13), 2071–2084.

Male, D.H., Gray, D.M., 1981. Handbook of Snow: Principles, Processes, Management and us Snow Cover Ablation and Runoff. Pergamon Press Canada Ltd, Toronto, Ont.

Marks, D., Cooley, K.R., Robertson, D.C., Winstral, A., 2001. Longterm snow database, Reynolds Creek Experimental Watershed, Idaho, United States. Water Resour. Res. 37 (11), 2835–2838.

Marks, D., Dozier, J., 1992. Climate and energy exchange at the snow surface in the alpine region of the Sierra Nevada: 2. Snow cover energy balance. Water Resour. Res. 28 (11), 3043–3054.

Martinec, J., 1986. Meltwater percolation through an alpine snowpack. Proceedings Davos Symposium - Avalanche Formation, Movement and Effects, vol. 162. IAH.

Meeks, J., Hunkeler, D., 2015. Snowmelt infiltration and storage within a karstic environment, Vers Chez le Brandt, Switzerland. J. Hydrol. 529, 11–21.

Melching, C.S., Yen, B.C., Wenzel, H.G., 1990. A reliability estimation in modeling watershed runoff with uncertainties. Water Resour. Res. 26 (10), 2275–2286.

Moeck, C., Hunkeler, D., Brunner, P., 2015. Tutorials as a flexible alternative to GUIs: an example for advanced model calibration using Pilot Points. Environ. Model. Softw. 66, 78–86.

Mualem, Y., 1976. A new model for predicting the hydraulic conductivity of unsaturated porous media. Water Resour. Res. 12 (3), 513–522.

Mullem, V.A., Garen, D., Woodward, D.E., 2004. Snowmelt. In: Agriculture, U.S.D.O., ed. Part 630 Hydrology - National Engineering Handbook.

Müller, I., 1978. La variabilité des caractéristiques physicochimiques des eaux dans la zone d'infiltration du karst jurassien et prealpin Congrès Suisse Spéléologie, vol. 16.09-18.09.1978 Porrentruy, pp. 131–137.

Müller, I., Schotterer, U., Siegenthaler, U., 1982. Etude des caractéristiques structurales et hydrodynamiques des aquifères karstiques par leur réponses naturelles et provoquées. Eclogae Geol. Helv. 95 (1).
Nash, J.E., Sutcliffe, J.V., 1970. River flow forecasting through conceptual models Part I—a discussion of principles. J. Hydrol. 10 (3), 282–290.
Ohmura, A., 2001. Physical basis for the temperature-based melt-index method. J. Appl. Meteorol. 40 (4), 753–761.
Pellicciotti, F., Brock, B., Strasser, U., Burlando, P., Funk, M., Corripio, J., 2005. An enhanced temperature-index glacier melt model including the shortwave radiation balance: development and testing for Haut Glacier d'Arolla, Switzerland. J. Glaciol. 51 (175), 573–587.
Prata, A., 1996. A new long-wave formula for estimating downward clear-sky radiation at the surface. Q. J. R. Meteorol. Soc. 122 (533), 1127–1151.
Rice, R., Bales, R.C., 2010. Embedded sensor network design for snow cover measurements around snow pillow and snow course sites in the Sierra Nevada of California. Water Resour. Res. 46 (3).
Rutter, N., Essery, R., Pomeroy, J., Altimir, N., Andreadis, K., Baker, I., Barr, A., Bartlett, P., Boone, A., Deng, H., 2009. Evaluation of forest snow processes models (SnowMIP2). J.Geophys. Res.: Atmos. (1984, Äì2012) 114 (D6).
Seibert, J., 1997. Estimation of parameter uncertainty in the HBV model. Hydrol. Res. 28 (4–5), 247–262.
Slater, A., Barrett, A., Clark, M., Lundquist, J., Raleigh, M., 2013. Uncertainty in seasonal snow reconstruction: relative impacts of model forcing and image availability. Adv. Water Resour. 55, 165–177.
Sommaruga, A., 1997. Geology of the central Jura and the molasse basin: new insight into an evaporite- based foreland fold and thrust beld. In: Naturelles, L.s. t.n.t.d.s., ed., vol. 12, Neuchatel, p. 175.
Sten, B.m., 1975. The development of a snow routine for the HBV-2 model. Nord. Hydrol. 6 (2), 73–92.
Strasser, U., Marke, T., 2010. ESCIMO. spread, a spreadsheet-based point snow surface energy balance model to calculate hourly snow water equivalent and melt rates for historical and changing climate conditions. Geosci. Model Dev. Discuss. 3 (2), 627–649.
Tekeli, A.E., Sorman, A., Sensoy, A., Sorman, A.U., Bonta, J., Schaefer, G., 2005. Snowmelt lysimeters for real-time snowmelt studies in Turkey. Turk. J. Eng. Environ. Sci. 29 (1), 29–40.
Tobin, C., Schaefli, B., Nictina, L., Simoni, S., Barrenetxea, G., Smith, R., Parlange, M., Rinaldo, A., 2013. Improving the degree-day method for sub-daily melt simulations with physically-based diurnal variations. Adv. Water Resour. 55, 149–164.
Tonkin, M., Doherty, J., 2009. Calibration-constrained Monte Carlo analysis of highly parameterized models using subspace techniques. Water Resour. Res. 45.
Tonkin, M.J., Doherty, J., 2005. A hybrid regularized inversion methodology for highly parameterized environmental models. Water Resour. Res. 41 (10).
Trujillo, E., Molotch, N., 2011. Snowpack regimes of the Western United States. Proceedings AGU Fall Meeting Abstracts 2011, vol. 1, p. 0684.
Valley, B., 2002. La vallée des Ponts-de–Martel: Rétro–déformation 3-D d'une structure complexe dans le Jura Neuchâtelois Master. University of Neuchatel, p. 107.
Van Genuchten, M.T., 1980. A closed-form equation for predicting the hydraulic conductivity of unsaturated soils. Soil Sci. Soc. Am. J. 44 (5), 892–898.
Watson, T.A., Doherty, J.E., Christensen, S., 2013. Parameter and predictive outcomes of model simplification. Water Resour. Res. 49 (7), 3952–3977.
Willmott, C.J., 1981. On the validation of models. Phys. Geogr. 2 (2), 184–194.
Yang, Z.-L., 2008. Description of recent snow models: snow and climate.